Supplementary Information

Vortex fluidic regulated phospholipid equilibria involving liposomes down to sub-micelle size assemblies

Nikita Joseph,[a,†] Marzieh Mirzamani,[b,†] Tarfah Abudiyah,[a] Ahmed Hussein Mohammed Al-Antaki,[a,c] Matt Jellicoe,[a] David P Harvey,[a] Emily Crawley,[a] Clarence Chuah,[a] Andrew E Whitten,[d] Elliot Paul Gilbert,[d] Shuo Qian,[e] Lilin He,[f] Michael Z. Michael,[g] Harshita Kumari,[b,*] Colin L Raston[a,*]

[a.] *Flinders Institute for Nanoscale Science and Technology (INST), College of Science and Technology, Flinders University, Bedford park, SA 5042 Australia*
[b.] *James L. Winkle College of Pharmacy, University of Cincinnati, Cincinnati, OH 45267-0004, USA.*
[c.] *Department of Chemistry, Faculty of Science, University of Kufa, Najaf 54001, Iraq.*
[d.] *Australian Nuclear Science and Technology Organization (ANSTO), Lucas Heights, NSW 2234 Australia.*
[e.] *The Second Target Station Project of SNS, Oak Ridge National Laboratory, Oak Ridge, TN 37830, USA.*
[f.] *Neutron Scattering Division, Oak Ridge National Laboratory, Oak Ridge, TN 37830, USA.*
[g.] *Flinders Centre for Innovation in Cancer (FCIC), Flinders Medical Centre (FMC), Bedford Park, SA 5042 Australia.*

† *Authors contributed equally to this work.*

*Corresponding Authors

Prof. Colin L Raston

Email: colin.raston@flinders.edu.au

Prof. Harshita Kumari

Email: kumariha@ucmail.uc.edu

Contents

1. General materials and methods.

All the chemicals were used as received unless otherwise stated. 1-Palmitoyl-2-oleoyl-sn-glycero-3-phosphocholine (POPC) was purchased from Sapphire Biosciences NSW 2016. Trichlorododecaylsilane $\geq 95.0\%$ (GC) for the treatment of hydrophobic surface of the glass tube was purchased from Sigma Aldrich NSW 2016. All the solutions were prepared at room temperature unless otherwise stated using Milli-Q water. 1,2-dipalmitoyl-sn-glycero-3-phosphoethanolamine-N-(7-nitro-2-1,3-benzoxadiazol-4-yl) (ammonium salt) 16:0 NBD-PE and 1,2-dipalmitoyl-sn-glycero-3-phosphoethanolamine-N-(lissamine rhodamine B sulfonyl) (ammonium salt) 16:0 (Liss Rh-PE) was purchased from Avanti Polar Lipids USA. All the samples for SANS experiments were prepared in 100% D_2O.

All the liposomes samples were analyzed by Dynamic Light Scattering (DLS) using particle sizer DLS (Nano ZS90, Malvern instruments, Worcester, UK). Scanning electron microscopy (SEM) was performed using a FEI Quanta 450, atomic force microscopy (AFM) using the Nanoscope 8.10 in tapping mode, Transmission Electron Microscopy (TEM) Samples were prepared by drop-casting the material onto standard carbon coated copper grids prior to characterization. Real-time SANS experiments were done at the Australian Nuclear Science and Technology Organization (ANSTO) and HFIR at ORNL using the Bilby and BioSANS instruments respectively.

2. Effect on the size of liposomes processed in hydrophobic tube.

Phospholipid suspensions at a concentration of 25 μg/mL were processed int the confined mode; 1 mL sample volumes were processed in a hydrophilic surface VFD tube titled at 45° and rotating at 9000 rpm. These were characterized using Dynamic Light Scattering (DLS) (Red) and compared with the same conditions in a hydrophobic surface tube (Green). After treating the VFD surface the size distribution changes from micron range (red) towards 100 nm (green) in size. The hydrophobic nature of the tube controls the self-assembly more towards the nm scale region.

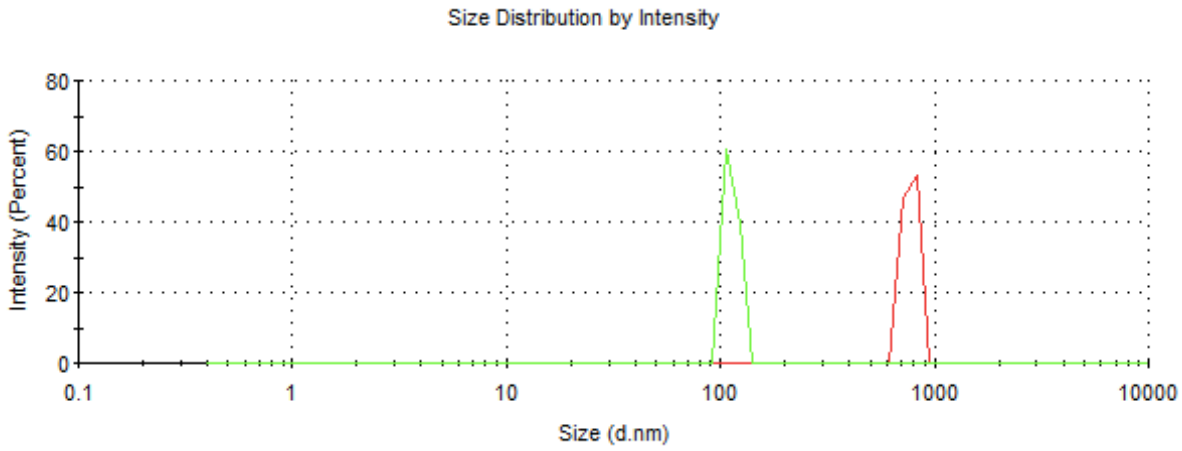

Fig S1: DLS of 1 mL of phospholipid suspension at 25 μg/mL were processed with the tube titled at 45° and rotating at 9000 rpm. All the samples were characterized at room temperature 25°C. The hydrophilic tube (uncoated) sample and hydrophobic tube sample are shown in green and red respectively. The glass tubes used were 20 mm in outside diameter.

3. Rotational speed optimization in hydrophobic tubes.

Phospholipid suspension at a concentration of 25 μg/mL was processed in continuous flow at a flow rate of 0.1 mL/min, with the hydrophobic coated tube tilted at 45° and rotated at 4000 rpm, 5000, 6000, 7000, 8000 and 9000 rpm. All the samples were characterized using DLS. The 9000 rpm rotational speed was deemed optimal, with a size range of 100 – 200 nm and PDI of 0.2 – 0.3.

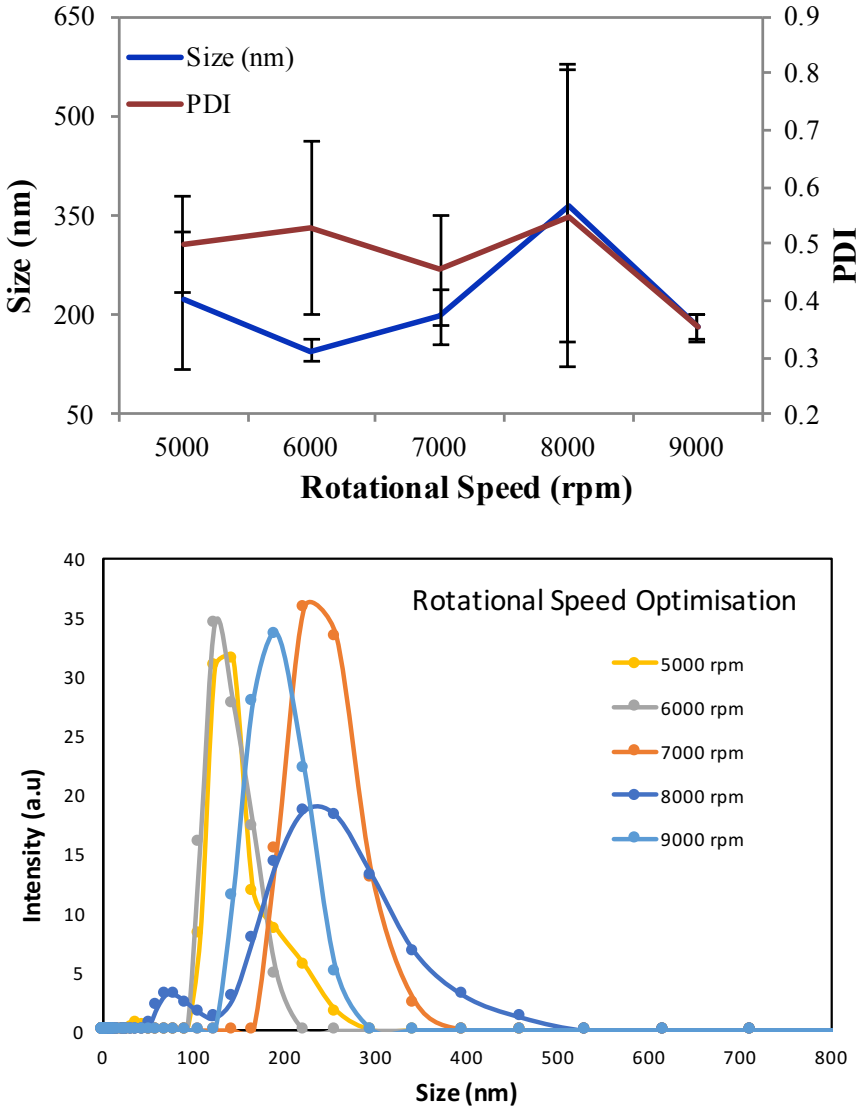

Fig S2: DLS at room temperature of phospholipid suspensions in water at a concentration of 25 µg/mL and processed under continuous flow at a flow rate of 0.1 mL/min, tilt angle 45° with the tube rotated at 4000, 5000, 6000, 7000, 8000 and 9000 rpm. All the sample measurements were repeated in triplicate and a standard error was obtained. All the samples were processed in hydrophobic coated inner surface tube with an OD of 20 mm.

4. Tilt angle optimization in hydrophobic tubes.

Phospholipid suspensions at a concentration of 25 μg/mL were processed under continuous flow in a hydrophobic tube, at a flow rate of 0.1 mL/min, with the tube rotating at 9000 rpm and tilted at 0°, 15°, 30°, 45°, 60° and 75°. All the samples were characterized by DLS. The optimal tilt angle was 45° which is also common for processing in general in the VFD.

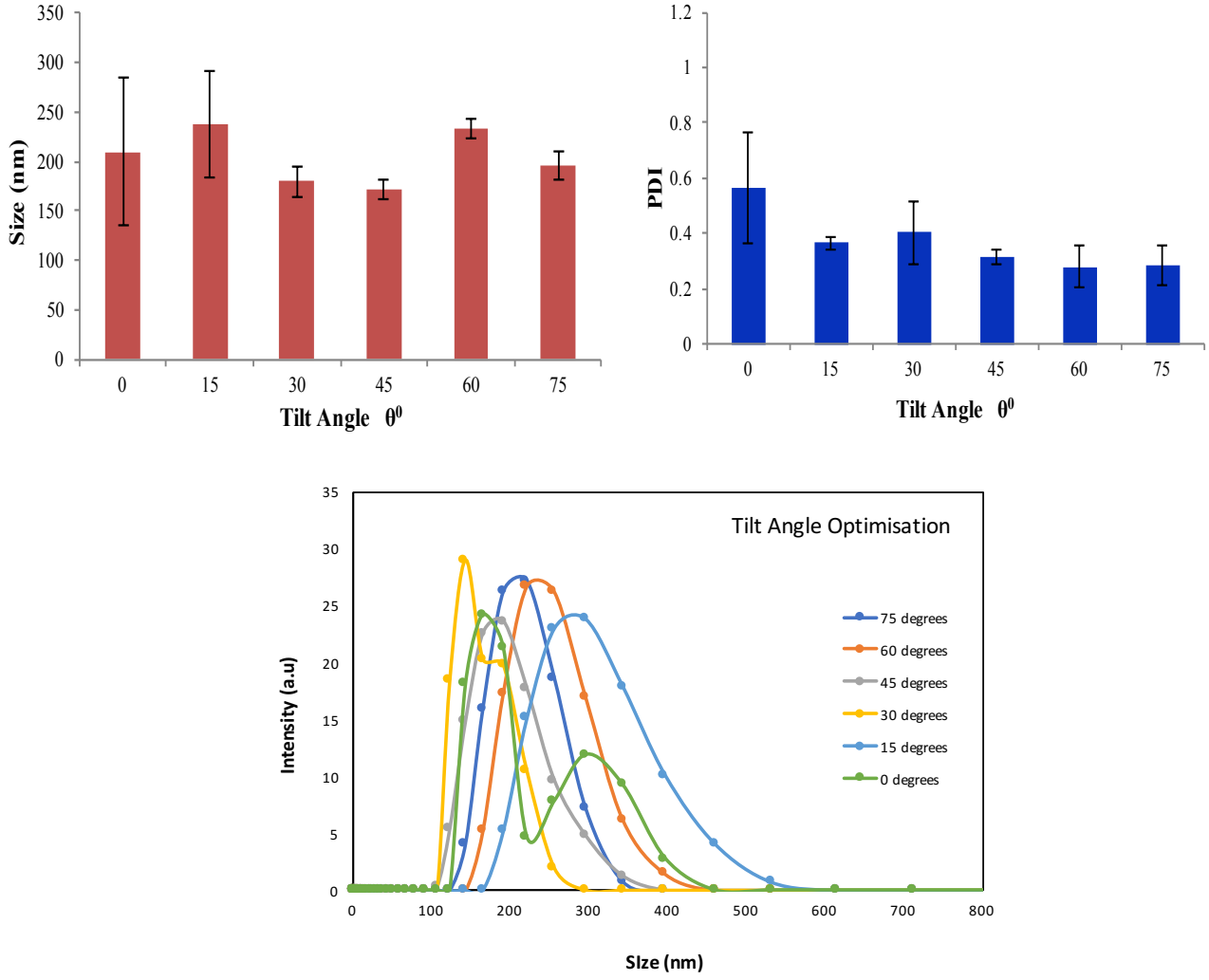

Fig S3: Phospholipid suspensions at a concentration of 25 μg/mL were processed under continuous flow at a flow rate of 0.1 mL/min, rotational speed 9000 rpm and tilt angles 0°, 15°, 30°, 45°, 60° and 75° . All the samples were characterized using DLS at room temperature 25°C for a hydrophobic tube 20 mm OD; all sample measurements were repeated in triplicate and a standard error was obtained.

5. Flow-rate optimization in hydrophobic tubes.

Phospholipid suspensions at a concentration of 25 μg/mL was processed at 9000 rpm in continuous flow at a hydrophobic tube tilted at 45° at flow-rates 0.1, 0.3, 0.5, 0.7 and 1.0 mL/min. The size was observed to be around 100 nm at the lowest flow rate 0.1 mL/min with low polydispersity index (PDI). The lower the flow-rate, the greater is the residence time for the samples to be processed under shear which impacts on the controlling the size of the self-assembled particles. All the measurements were studied using DLS.

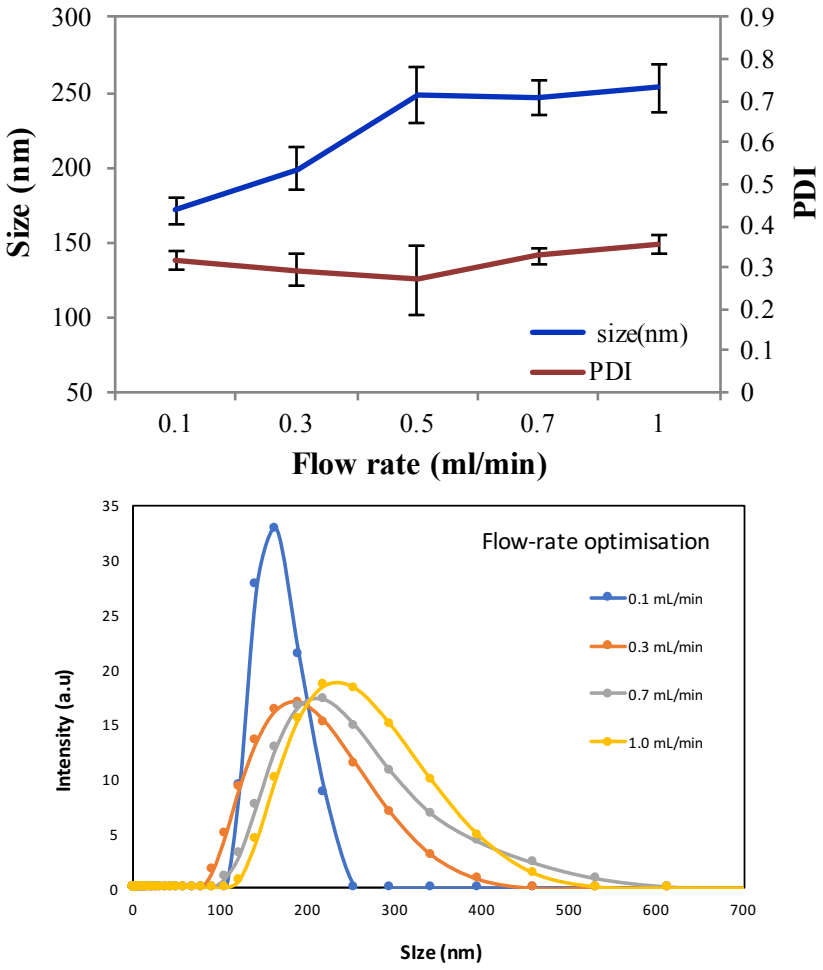

Fig S4: Phospholipid suspensions at a concentration of 25 μg/mL was processed at 9000 rpm under continuous flow in a hydrophobic coated tube, 20 mm OD, tilt angle 45°, flow-rates 0.1, 0.3, 0.5, 0.7 and 1.0 mL/min. All the samples were characterized using DLS at room temperature 25°C and the experiments were repeated in triplicates and a standard error obtained.

6. Concentration optimization in hydrophobic tubes.

Phospholipid suspensions at concentrations of 25, 50 and 1 mg/mL were processed under confined mode in the VFD, with the hydrophobic tube rotating at 9000 rpm and titled at 45°. All samples resulted in `100 nm diameter liposomes, using DLS, with the polydispersity (PDI) different at different concentrations, being the lowest for 25µg/mL. Different formulations in industry requires liposomal formulations at 0.1 – 1 mg/mL depending on the application.

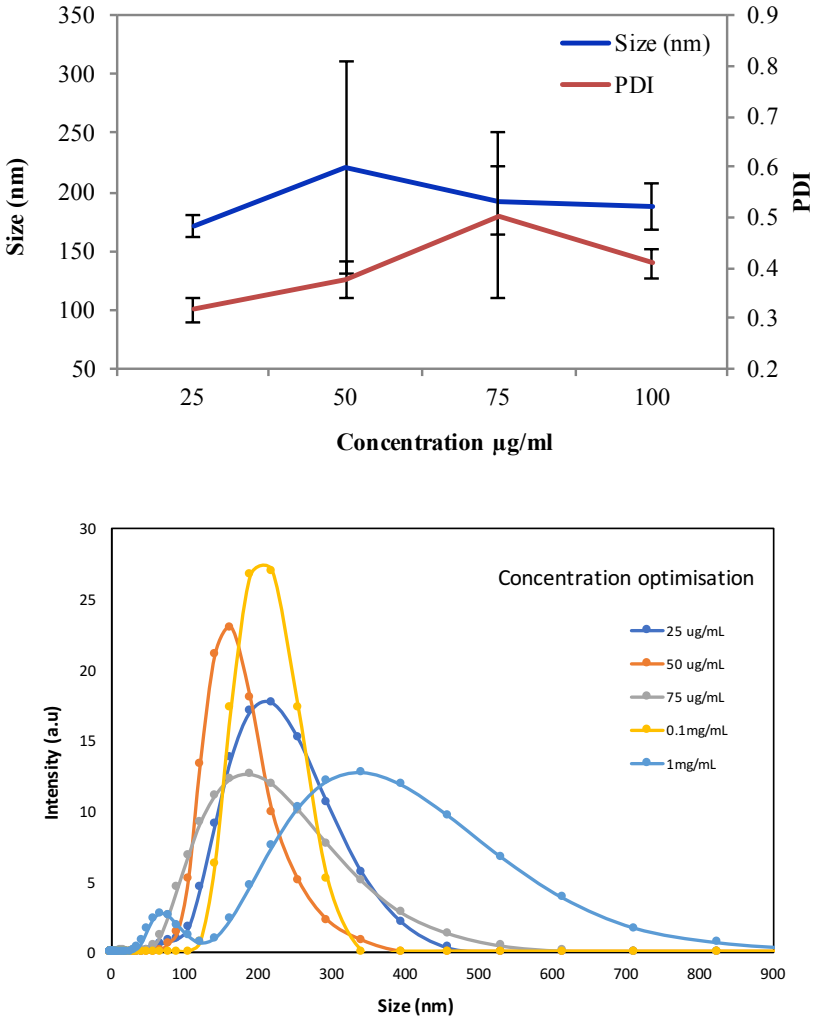

Fig S5: DLS of phospholipid suspensions at a concentration of 25, 50 and 1 mg/mL processed in confined mode in the VFD in a hydrophobic tube 20 mm OD rotating at 9000 rpm and tilted at 45°. All the samples were characterized at room temperature 25°C. All the sample measurements were repeated in triplicate and a standard error was obtained.

7. Transmission Electron Microscopy (TEM) of liposomes processed in bench top vortexer.

Phospholipid suspensions, 1 mg/mL, were vortexed in a vortex mixer for 15 minutes at room temperature and characterized using Transmission Electron Microscopy (TEM) as a control experiment. Similar samples was observed with non-uniform sizes of particles across the TEM grids. The liposomes processed from the vortexer were highly unstable under vacuum and were squeezed in size as observed from the images provided.

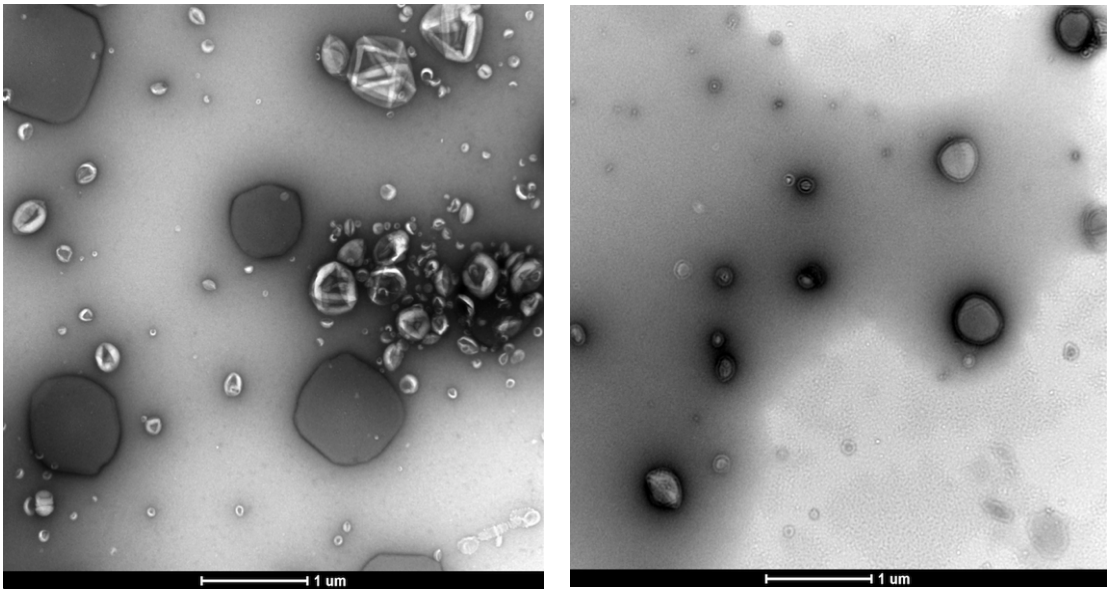

Fig S6: TEM images of material obtained from processing a phospholipid suspension, 1 mg/mL, in a vortex mixer for 15 minutes at room temperature. The TEM grid was pre plasma modified to generate a hydrophilic surface to obtain a better adherence of the sample. The sample was further stained by treating with 2% uranyl acetate and washing (x3) with Milli-Q water.

8. Small Angle Neutron Scattering Analysis (SANS).

Methods:

SANS data were analyzed using the NIST macros developed for Igor Pro. A variety of models were tested to determine the best fit, including lamellar, vesicle, and sphere form factors, as well as simpler empirical models. The fitting parameters for the best fit to each data set is shown below. Non-resolution-smeared models were used. Errors of 0 indicate that the parameter was held at a certain value and thus not fitted.

8a. ANSTO Data (inner surface of tube with hydrophobic coating)

POPC in D_2O, 0 RPM/unsheared (Power Law + Lorentzian Peak Summed Model)

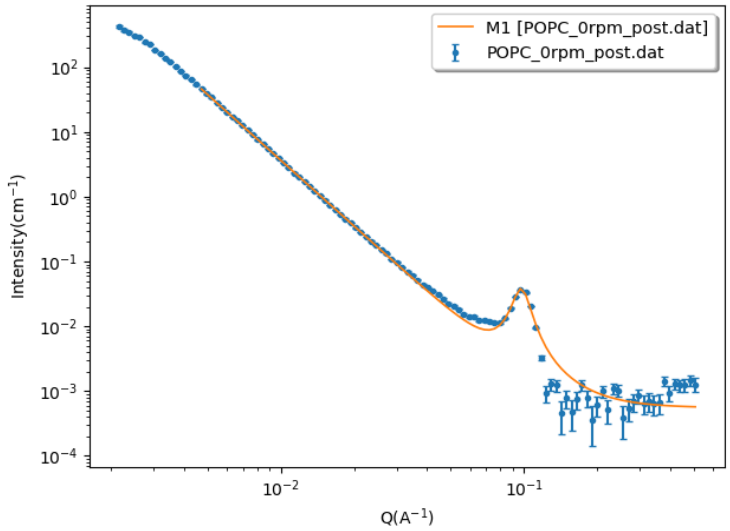

Scale	1.00	±	0
Background	5.49E-04	±	4.35E-05
Power Scale	6.68E-07	±	5.09E-09
Power	3.37	±	1.61E-03
Peak Scale	0.04	±	3.02E-04
Peak Position	0.10	±	6.93E-05
Peak HWHM	8.39E-03	±	1.03E-04
Range	0.0045	< q <	0.50833
Sqrt(χ^2/N)	4.3065		

POPC in D_2O, 3000 RPM, real-time shear (Power Law + Lorentzian Peak Summed Model)

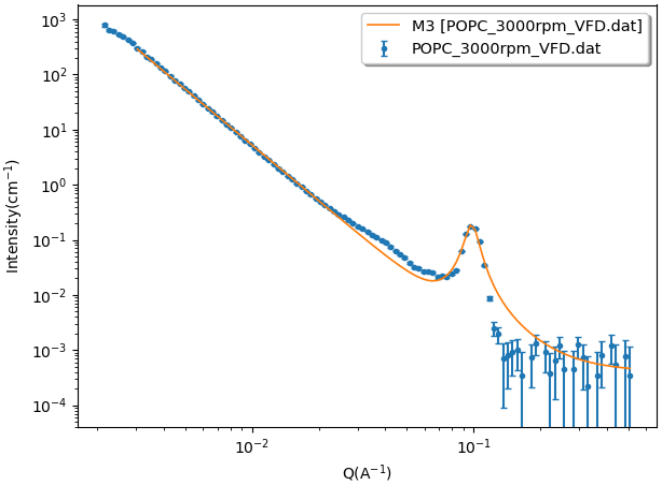

Scale	1.00	±	0
Background	4.00E-04	±	0
Power Scale	9.99E-07	±	1.07E-08
Power	3.36	±	2.21E-03
Peak Scale	0.19	±	9.71E-04
Peak Position	0.10	±	3.33E-05
Peak HWHM	6.91E-03	±	4.67E-05
Range	0.003	< q <	0.50833
Sqrt(χ^2/N)	7.4510		

POPC in D_2O, 3000 RPM, after shear (Power Law + Lorentzian Peak Summed Model)

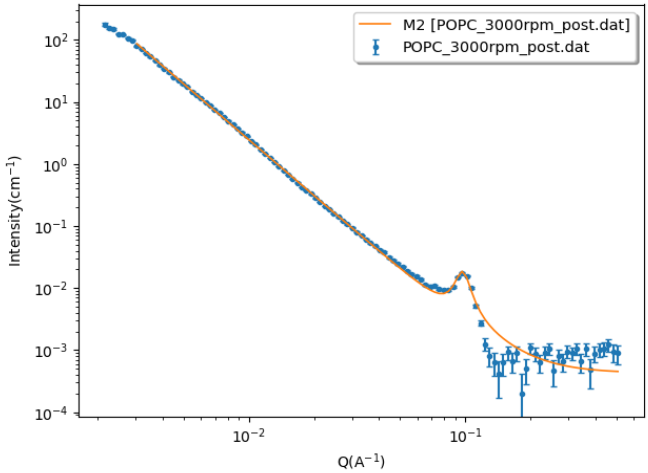

Scale	1.00	±	0
Background	4.29E-04	±	4.40E-05
Power Scale	2.63E-06	±	1.96E-08
Power	2.99	±	1.57E-03
Peak Scale	0.02	±	2.98E-04
Peak Position	0.10	±	1.58E-04
Peak HWHM	8.16E-03	±	2.34E-04
Range	0.003	< q <	0.50833
Sqrt(χ^2/N)	5.4896		

POPC in D_2O, 3800 RPM, real-time shear (Power Law + Lorentzian Peak Summed Model)

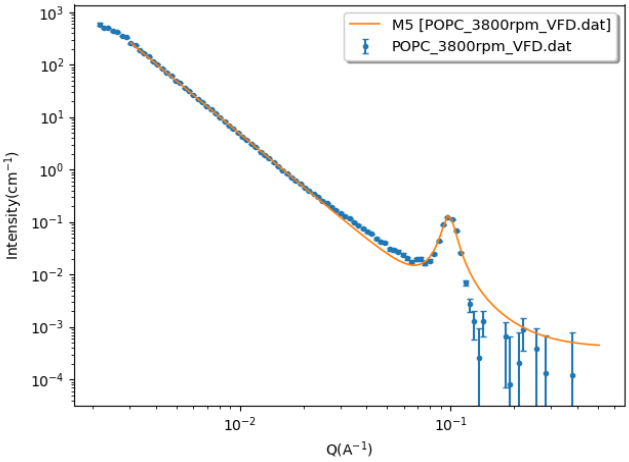

Scale	1.00	±	0
Background	4.00E-04	±	0
Power Scale	9.73E-07	±	1.19E-08
Power	3.35	±	2.51E-03
Peak Scale	0.13	±	9.99E-04
Peak Position	0.10	±	5.06E-05
Peak HWHM	7.05E-03	±	7.22E-05
Range	0.003	< q <	0.50833
Sqrt(χ^2/N)	4.6606		

POPC in D_2O, 3800 RPM, after shear (Power Law + Lorentzian Peak Summed Model)

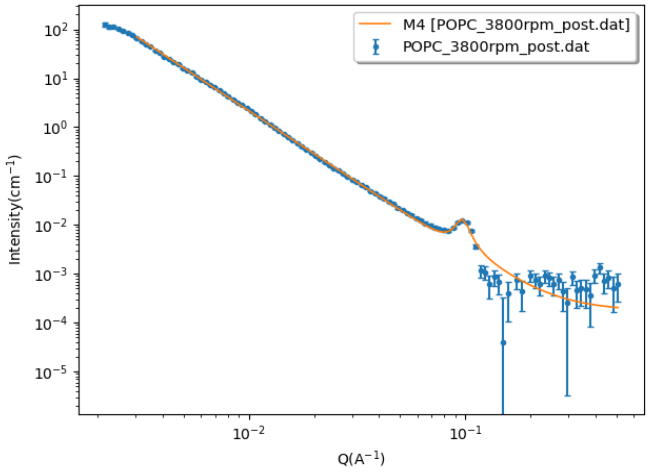

Scale	1.00	±	0
Background	1.78E-04	±	5.26E-05
Power Scale	3.20E-06	±	3.36E-08
Power	2.91	±	2.22E-03
Peak Scale	0.01	±	3.53E-04
Peak Position	0.10	±	2.92E-04
Peak HWHM	8.20E-03	±	4.32E-04
Range	0.003	< q <	0.50833
Sqrt(χ^2/N)	3.2924		

POPC in D_2O, 4000 RPM, real-time shear (Power Law + Lorentzian Peak Summed Model)

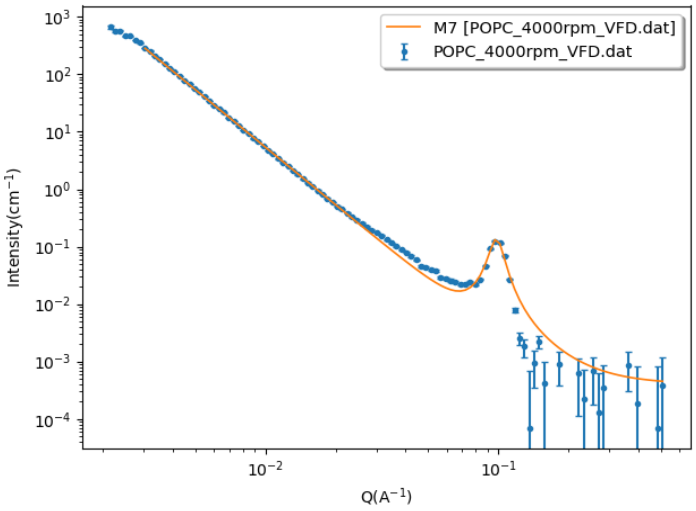

Scale	1.00	±	0
Background	4.00E-04	±	0
Power Scale	1.20E-06	±	1.20E-08
Power	3.33	±	2.05E-03
Peak Scale	0.13	±	8.78E-04
Peak Position	0.10	±	4.52E-05
Peak HWHM	7.25E-03	±	6.43E-05
Range	0.003	< q <	0.50833
Sqrt(χ^2/N)	5.6872		

POPC in D_2O, 4000 RPM, after shear (Power Law + Lorentzian Peak Summed Model)

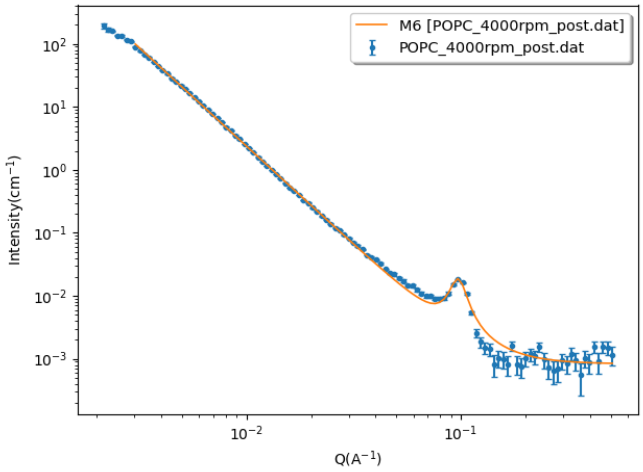

Scale	1.00	±	0
Background	8.31E-04	±	5.47E-05
Power Scale	1.34E-06	±	1.45E-08
Power	3.12	±	2.26E-03
Peak Scale	0.02	±	3.54E-04
Peak Position	0.10	±	1.99E-04
Peak HWHM	9.02E-03	±	2.98E-04
Range	0.003	< q <	0.50833
Sqrt(χ^2/N)	3.4807		

POPC in D_2O, 4500 RPM, real-time shear (Power Law + Lorentzian Peak Summed Model)

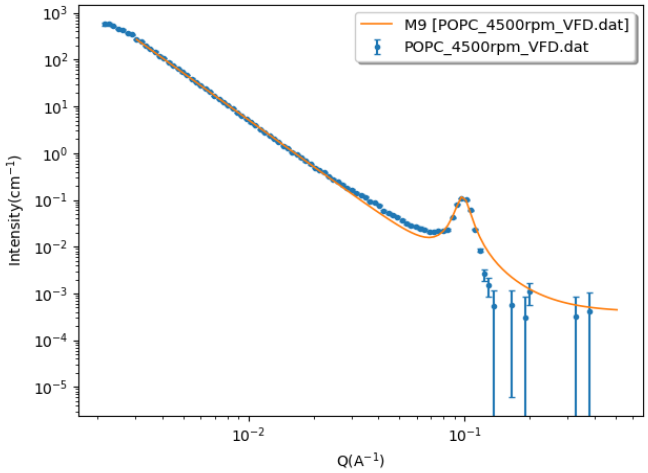

Scale	1.00	±	0
Background	4.00E-04	±	0
Power Scale	1.19E-06	±	1.26E-08
Power	3.32	±	2.17E-03
Peak Scale	0.12	±	8.96E-04
Peak Position	0.10	±	5.36E-05
Peak HWHM	7.30E-03	±	7.64E-05
Range	0.003	< q <	0.50833
Sqrt(χ^2/N)	4.9645		

POPC in D_2O, 4500 RPM, after shear (Power Law + Lorentzian Peak Summed Model)

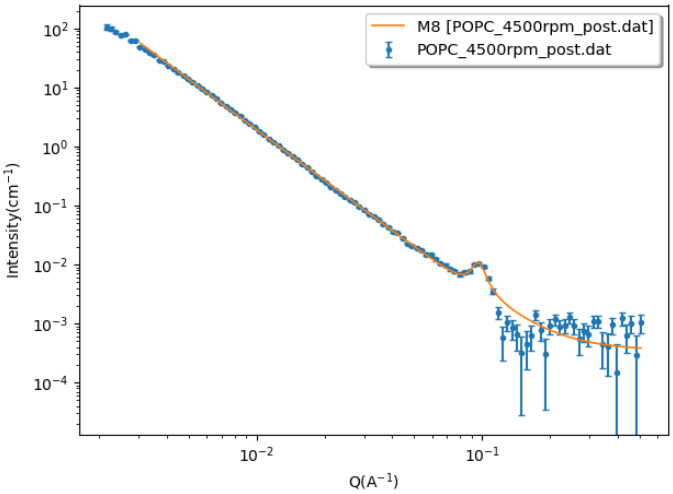

Scale	1.00	±	0
Background	3.54E-04	±	5.27E-05
Power Scale	3.95E-06	±	4.43E-08
Power	2.84	±	2.38E-03
Peak Scale	0.01	±	3.71E-04
Peak Position	0.10	±	3.63E-04
Peak HWHM	7.36E-03	±	5.23E-04
Range	0.003	< q <	0.50833
Sqrt(χ^2/N)	2.9460		

POPC in D_2O, 5000 RPM, real-time shear (Power Law + Lorentzian Peak Summed Model)

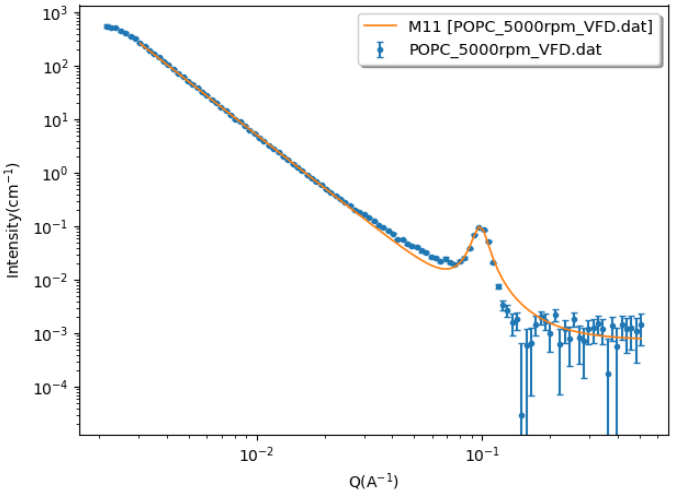

Scale	1.00	±	0
Background	7.52E-04	±	1.17E-04
Power Scale	1.29E-06	±	1.42E-08
Power	3.30	±	2.27E-03
Peak Scale	0.10	±	8.93E-04
Peak Position	0.10	±	6.80E-05
Peak HWHM	7.69E-03	±	1.02E-04
Range	0.003	< q <	0.50833
Sqrt(χ^2/N)	4.1391		

POPC in D_2O, 5000 RPM, after shear (Power Law + Lorentzian Peak Summed Model)

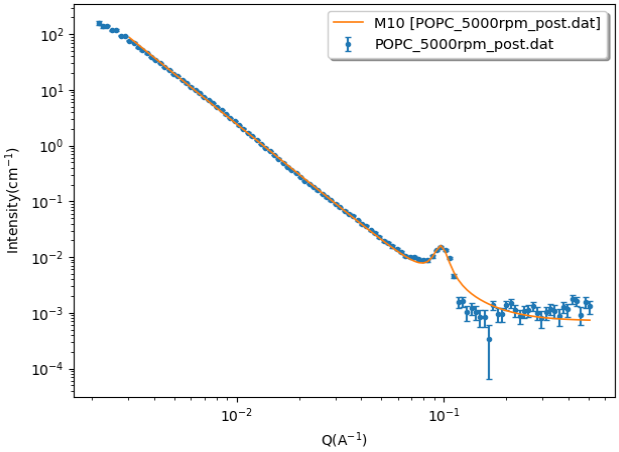

Scale	1.00	±	0
Background	7.15E-04	±	5.27E-05
Power Scale	2.48E-06	±	2.45E-08
Power	3.00	±	2.09E-03
Peak Scale	0.01	±	3.59E-04
Peak Position	0.10	±	2.30E-04
Peak HWHM	8.08E-03	±	3.41E-04
Range	0.003	< q <	0.50833
Sqrt(χ^2/N)	3.9784		

POPC in D_2O, 6000 RPM, real-time shear (Power Law + Lorentzian Peak Summed Model)

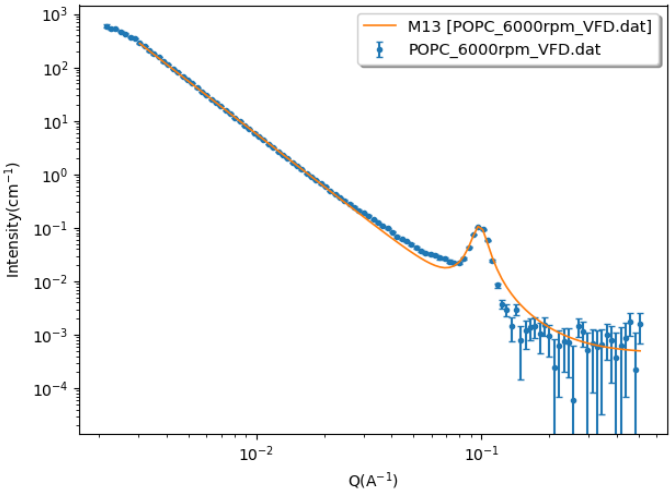

Scale	1.00	±	0
Background	4.46E-04	±	1.21E-04
Power Scale	1.69E-06	±	1.71E-08
Power	3.26	±	2.08E-03
Peak Scale	0.11	±	9.14E-04
Peak Position	0.10	±	6.45E-05
Peak HWHM	7.75E-03	±	9.72E-05
Range	0.003	< q <	0.50833
Sqrt(χ^2/N)	4.4328		

POPC in D_2O, 6000 RPM, after shear (Power Law + Lorentzian Peak Summed Model)

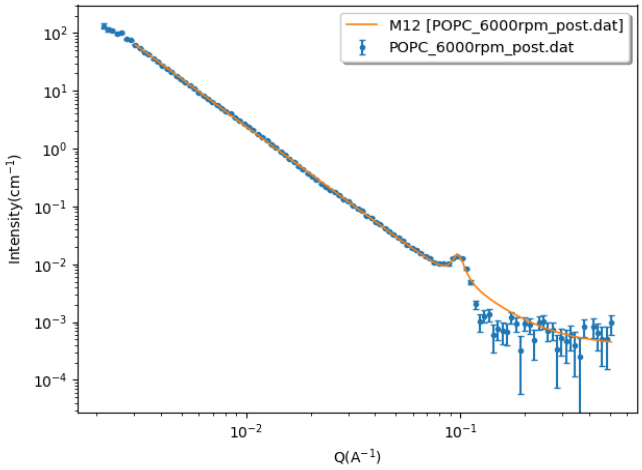

Scale	1.00	±	0
Background	4.00E-04	±	0
Power Scale	8.29E-06	±	7.49E-08
Power	2.73	±	1.95E-03
Peak Scale	0.01	±	4.02E-04
Peak Position	0.10	±	2.63E-04
Peak HWHM	6.41E-03	±	3.69E-04
Range	0.003	< q <	0.50833
Sqrt(χ^2/N)	3.6908		

POPC in D_2O, 7000 RPM, real-time shear (Power Law + Lorentzian Peak Summed Model)

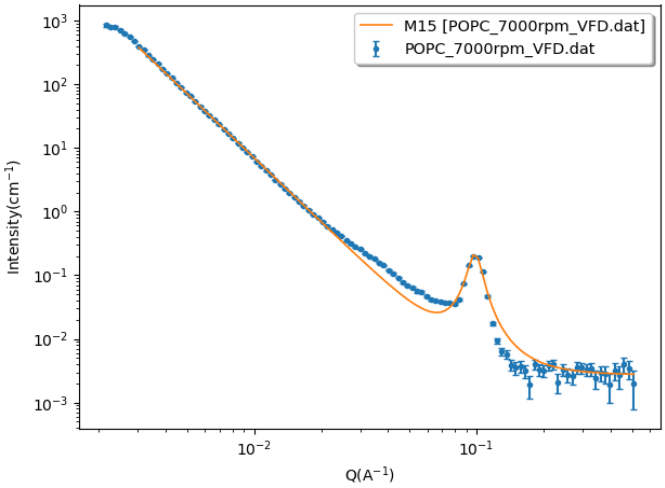

Scale	1.00	±	0
Background	2.71E-03	±	1.48E-04
Power Scale	1.44E-06	±	1.34E-08
Power	3.34	±	1.90E-03
Peak Scale	0.21	±	1.17E-03
Peak Position	0.10	±	3.85E-05
Peak HWHM	7.39E-03	±	5.86E-05
Range	0.003	< q <	0.50833
Sqrt(χ^2/N)	7.6663		

POPC in D_2O, 7000 RPM, after shear (Power Law + Lorentzian Peak Summed Model)

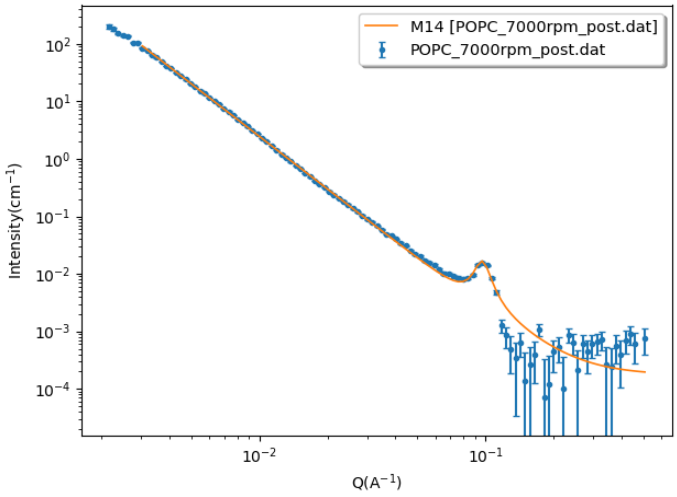

Scale	1.00	±	0
Background	1.75E-04	±	5.25E-05
Power Scale	2.09E-06	±	2.09E-08
Power	3.03	±	2.10E-03
Peak Scale	0.01	±	3.55E-04
Peak Position	0.10	±	2.11E-04
Peak HWHM	8.28E-03	±	3.11E-04
Range	0.003	< q <	0.50833
Sqrt(χ^2/N)	3.2356		

POPC in D_2O, 8000 RPM, real-time shear (Power Law + Lorentzian Peak Summed Model)

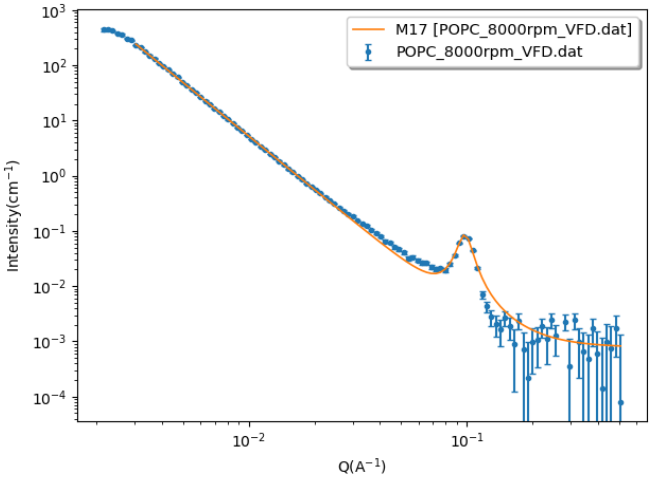

Scale	1.00	±	0	
Background	7.79E-04	±	1.55E-04	
Power Scale	1.94E-06	±	2.19E-08	
Power	3.21	±	2.29E-03	
Peak Scale	0.08	±	1.08E-03	
Peak Position	0.10	±	1.04E-04	
Peak HWHM	7.96E-03	±	1.57E-04	
Range	0.003	< q <	0.50833	
Sqrt(χ^2/N)	7.6663			3.0395

POPC in D_2O, 8000 RPM, after shear (Power Law + Lorentzian Peak Summed Model)

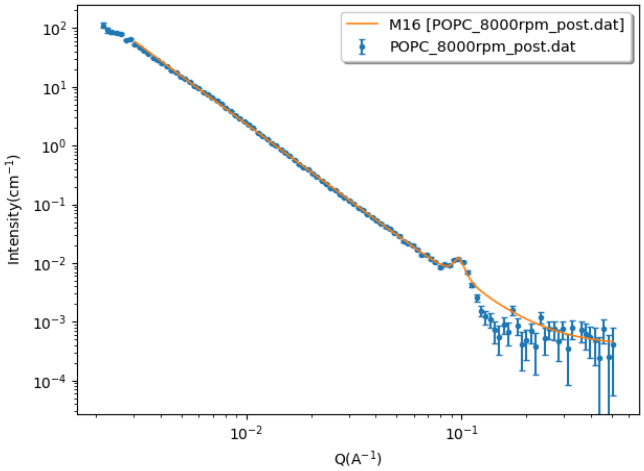

Scale	1.00	±	0
Background	4.00E-04	±	0
Power Scale	8.97E-06	±	8.18E-08
Power	2.71	±	1.97E-03
Peak Scale	0.01	±	4.03E-04
Peak Position	0.10	±	3.64E-04
Peak HWHM	6.01E-03	±	4.80E-04
Range	0.003	< q <	0.50833
Sqrt(χ^2/N)	3.4880		

POPC in D_2O, 9000 RPM, real-time shear (Power Law + Lorentzian Peak Summed Model)

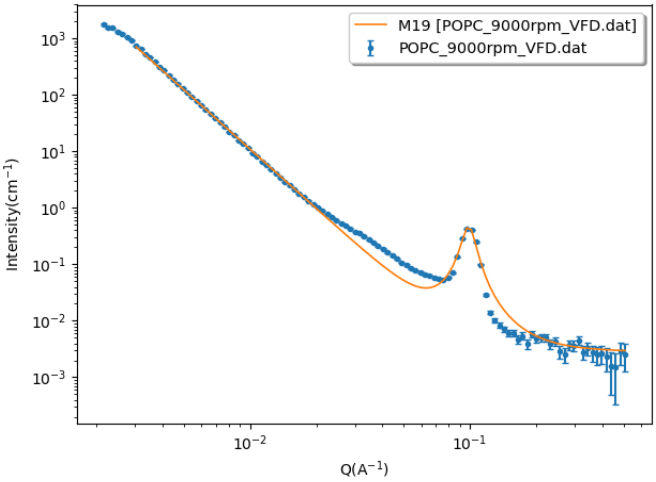

Scale	1.00	±	0	
Background	2.82E-03	±	1.57E-04	
Power Scale	1.13E-06	±	7.81E-09	
Power	3.49	±	1.40E-03	
Peak Scale	0.47	±	1.36E-03	
Peak Position	0.10	±	1.90E-05	
Peak HWHM	7.07E-03	±	2.90E-05	
Range	0.003	< q <	0.50833	
Sqrt(χ^2/N)	14.0943			3.0395

POPC in D_2O, 9000 RPM, after shear (Power Law + Lorentzian Peak Summed Model)

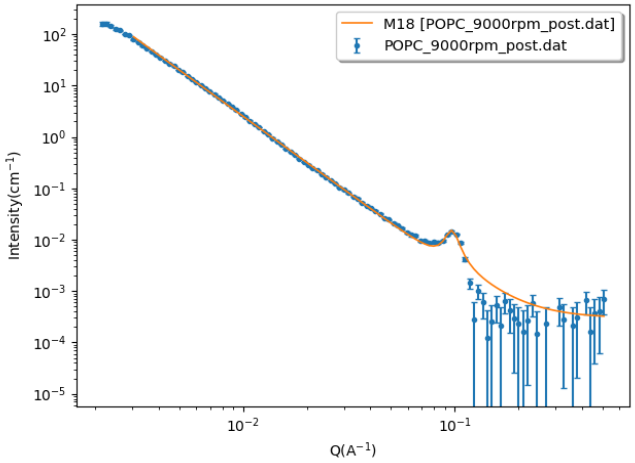

Scale	1.00	±	0
Background	3.00E-04	±	0
Power Scale	2.67E-06	±	2.56E-08
Power	2.99	±	2.02E-03
Peak Scale	0.01	±	3.63E-04
Peak Position	0.10	±	2.42E-04
Peak HWHM	7.97E-03	±	3.39E-04
Range	0.003	< q <	0.50833
Sqrt(χ^2/N)	4.0222		

8b. ORNL Data (uncoated tube)

POPC in D_2O, 3800 RPM, real-time shear (Power Law + Lorentzian Peak Summed Model)

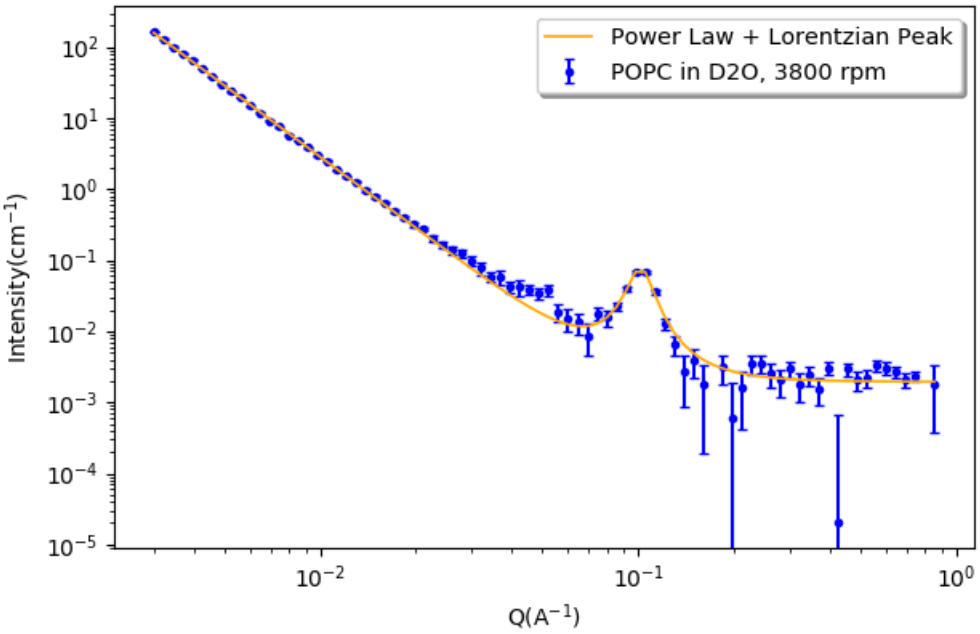

Scale	1	±	0
Background	1.94E-03	±	1.38E-04
Power Scale	6.05E-07	±	2.51E-08
Power	3.34	±	8.01E-03
Peak Scale	0.08	±	3.06E-03
Peak Position	0.10	±	3.26E-04
Peak HWHM	9.05E-03	±	5.15E-04
Range	.003	< q <	0.8544
Sqrt(χ^2/N)	1.6858		

POPC in D_2O, 4000 RPM, real-time shear (Power Law + Lorentzian Peak Summed Model)

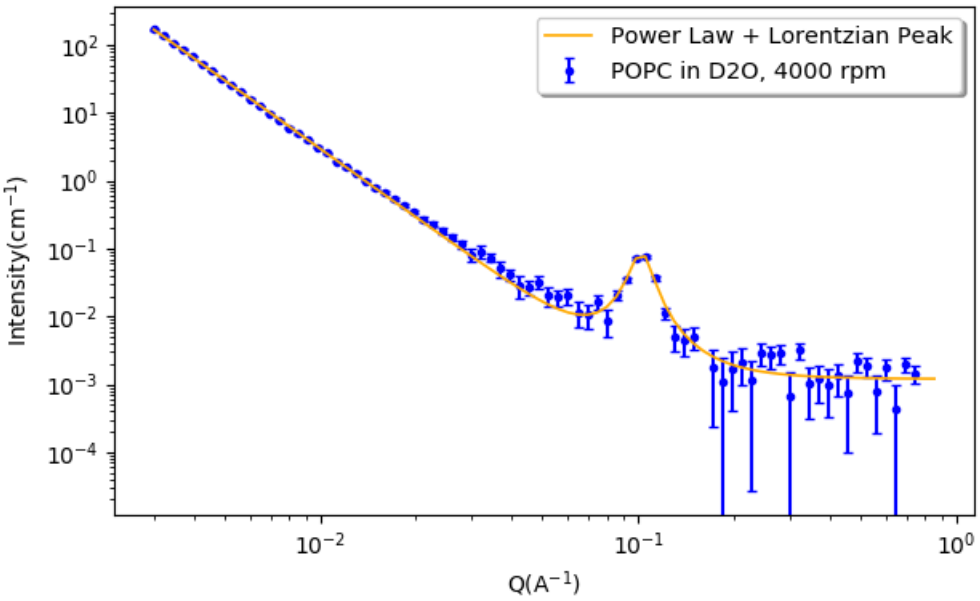

Scale	1	±	0
Background	1.20E-03	±	1.40E-04
Power Scale	5.77E-07	±	2.34E-08
Power	3.36	±	7.82E-03
Peak Scale	0.09	±	3.40E-03
Peak Position	0.10	±	2.74E-04
Peak HWHM	8.13E-03	±	4.52E-04
Range	.003	< q <	0.8544
Sqrt(χ^2/N)	1.4338		

POPC in D_2O, 4500 RPM, real-time shear (Power Law + Lorentzian Peak Summed Model)

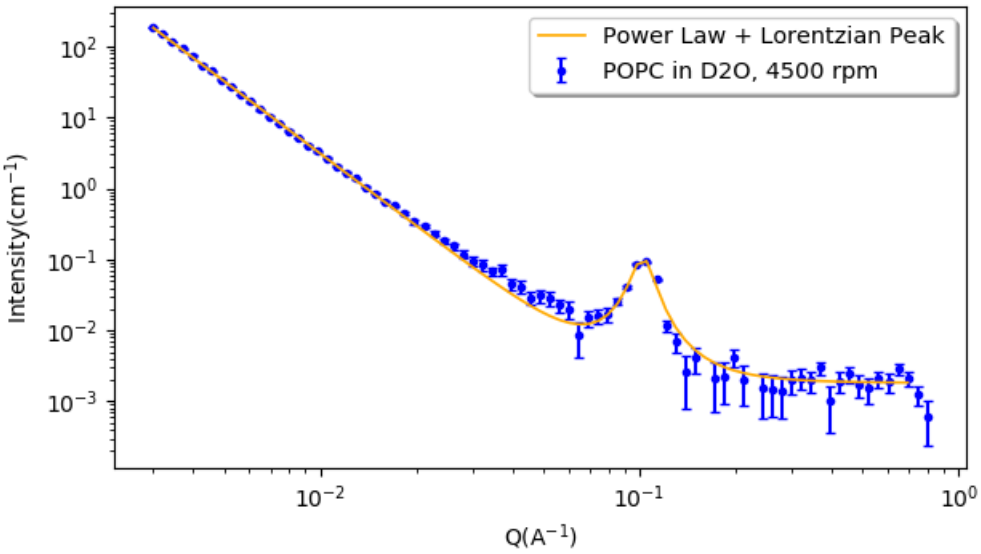

Scale	1	±	0
Background	1.82E-03	±	1.53E-04
Power Scale	5.24E-07	±	1.95E-08
Power	3.39	±	7.18E-03
Peak Scale	0.10	±	3.17E-03
Peak Position	0.10	±	2.26E-04
Peak HWHM	8.34E-03	±	3.57E-04
Range	.003	< q <	0.72
Sqrt(χ^2/N)	1.8314		

POPC in D_2O, 5000 RPM, real-time shear (Power Law + Lorentzian Peak Summed Model)

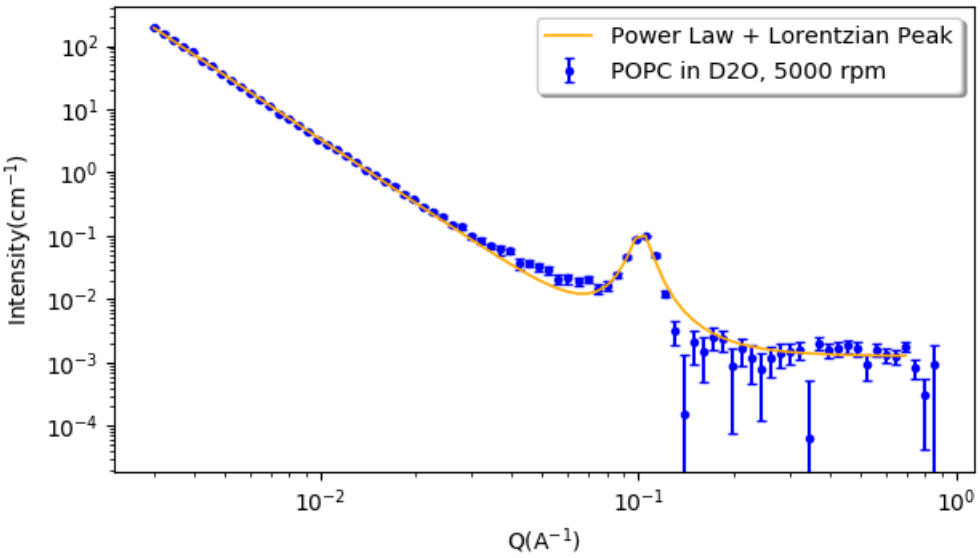

Scale	1	±	0
Background	1.26E-03	±	1.02E-04
Power Scale	6.47E-07	±	1.93E-08
Power	3.36	±	5.80E-03
Peak Scale	0.11	±	2.61E-03
Peak Position	0.10	±	1.47E-04
Peak HWHM	7.78E-03	±	2.37E-04
Range	.003	< q <	0.72
Sqrt(χ^2/N)	2.3230		

POPC in D_2O, 6000 RPM, real-time shear (Power Law + Lorentzian Peak Summed Model)

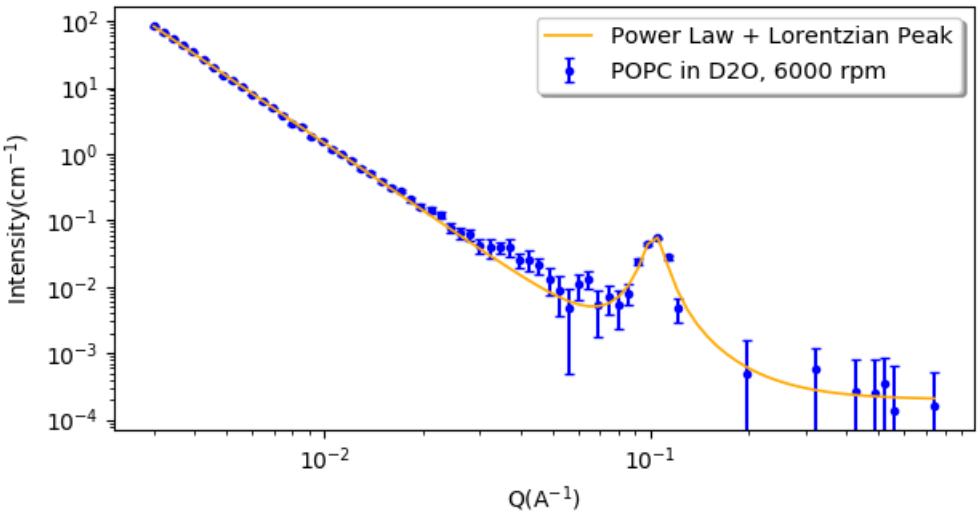

Scale	1	±	0
Background	2.00E-04	±	0
Power Scale	2.81E-07	±	1.78E-08
Power	3.36	±	1.22E-02
Peak Scale	0.06	±	3.13E-03
Peak Position	0.10	±	3.20E-04
Peak HWHM	7.23E-03	±	5.06E-04
Range	.003	< q <	0.75
Sqrt(χ^2/N)	1.5679		

POPC in D_2O, 7000 RPM, real-time shear (Power Law + Lorentzian Peak Summed Model)

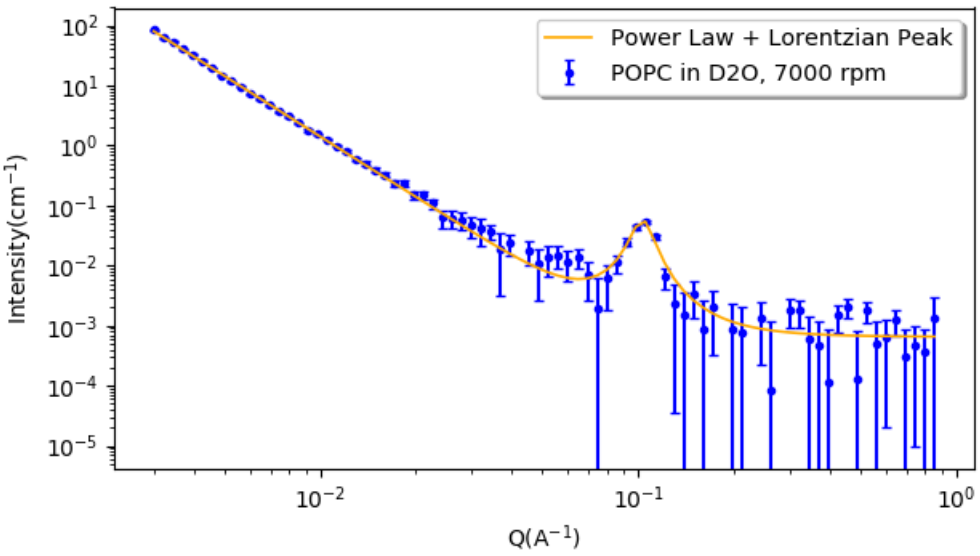

Scale	1	±	0
Background	6.51E-04	±	1.57E-04
Power Scale	2.82E-07	±	2.36E-08
Power	3.35	±	1.62E-02
Peak Scale	0.06	±	3.40E-03
Peak Position	0.10	±	4.84E-04
Peak HWHM	8.42E-03	±	7.01E-04
Range	.003	< q <	0.8544
Sqrt(χ^2/N)	1.1496		

POPC in D_2O, 8000 RPM, real-time shear (Power Law + Lorentzian Peak Summed Model)

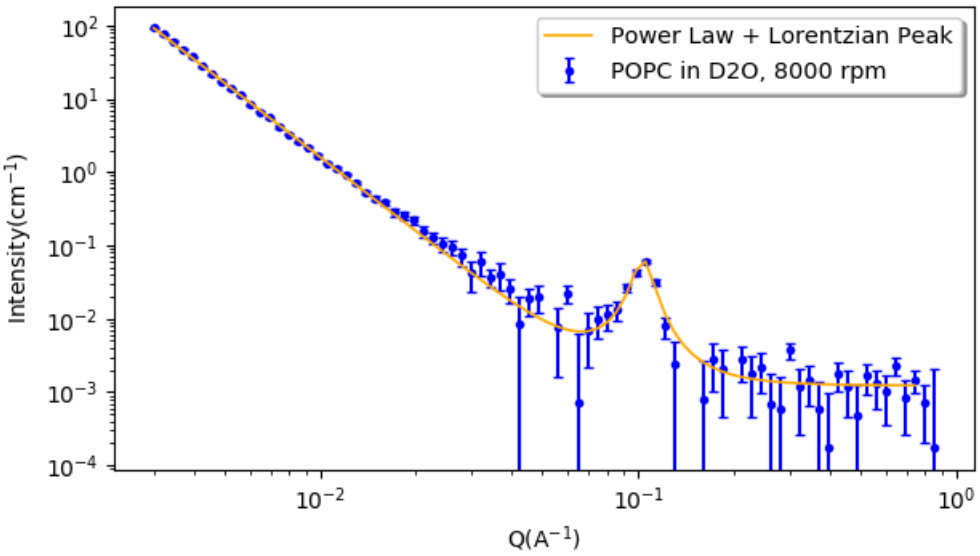

Scale	1	±	0
Background	1.22E-03	±	1.75E-04
Power Scale	3.01E-07	±	2.29E-08
Power	3.36	±	1.46E-02
Peak Scale	0.06	±	3.55E-03
Peak Position	0.10	±	4.72E-04
Peak HWHM	7.89E-03	±	6.32E-04
Range	.003	< q <	0.77
Sqrt(χ^2/N)	1.2307		

POPC in D_2O, 9000 RPM, real-time shear (Power Law + Lorentzian Peak Summed Model)

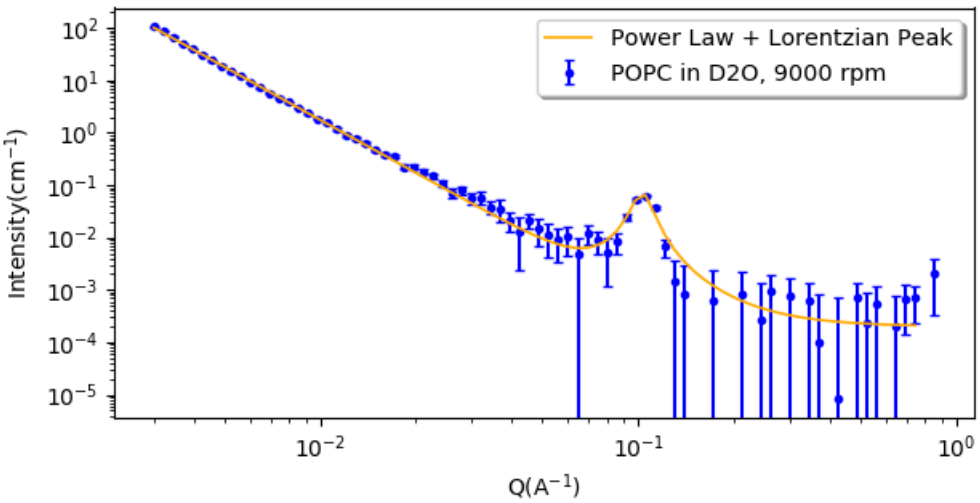

Scale	1	±	0
Background	2.00E-04	±	0.00E+00
Power Scale	3.32E-07	±	2.19E-08
Power	3.36	±	1.27E-02
Peak Scale	0.07	±	3.66E-03
Peak Position	0.10	±	3.78E-04
Peak HWHM	7.79E-03	±	5.58E-04
Range	.003	< q <	0.77
Sqrt(χ^2/N)	1.3976		